© 2014. Published by The Company of Biologists Ltd | Development (2014) 141, 2014-2023 doi:10.1242/dev.104240

RESEARCH ARTICLE

STEM CELLS AND REGENERATION

Sara endosomes and the asymmetric division of intestinal stem cells

Chrystelle Montagne and Marcos Gonzalez-Gaitan*

ABSTRACT

Tissue homeostasis is maintained by adult stem cells, which self-renew and give rise to differentiating cells. The generation of daughter cells with different fates is mediated by signalling molecules coming from an external niche or being asymmetrically dispatched between the two daughters upon stem cell mitosis. In the adult *Drosophila* midgut, the intestinal stem cell (ISC) divides to generate a new ISC and an enteroblast (EB) differentiating daughter. Notch signalling activity restricted to the EB regulates intestinal cell fate decision. Here, we show that ISCs divide asymmetrically, and Sara endosomes in ISCs are specifically dispatched to the presumptive EB. During ISC mitosis, Notch and Delta traffic through Sara endosomes, thereby contributing to Notch signalling bias, as revealed in Sara mutants: Sara itself contributes to the control of the ISC asymmetric division. Our data uncover an intrinsic endosomal mechanism during ISC mitosis, which participates in the maintenance of the adult intestinal lineage.

KEY WORDS: Sara endosomes, Notch signalling, Intestinal stem cells

INTRODUCTION

Adult stem cells have the capacity to self-renew indefinitely and to generate differentiated cells to maintain and repair the tissue in which they are located. The formation of daughter cells with distinct developmental potentials depends on two major mechanisms: the regulation by a stem cell niche and/or the asymmetric distribution of cell fate determinants (Morrison and Spradling, 2008; Hsu and Fuchs, 2012). The unequal segregation of cell fate determinants is achieved by several processes: (1) the polarization of the mother cell; (2) the orientation of the mitotic spindle with respect to the polarity axes of the mother cell; and (3) the asymmetric partitioning of signalling molecules (reviewed by Fürthauer and González-Gaitán, 2009a). The directional targeting of signalling molecules to one of the two daughter cells leads to the adoption of a specialized cell fate.

Several years ago, intestinal stem cells were discovered in the adult *Drosophila* midgut (Micchelli and Perrimon, 2006; Ohlstein and Spradling, 2006). The epithelium of the fly digestive system is composed of four cell types: the intestinal stem cell (ISC), the transient enteroblast (EB), the enterocyte (EC) (which is required for the absorption of nutrients and water) and the enteroendocrine cell (ee), which secretes hormones facilitating digestion in the midgut. Upon mitosis, ISC generates a new stem cell and an EB, which is committed to differentiation. EBs undergo differentiation into either ECs or ees (Ohlstein and Spradling, 2007).

ISCs could in principle divide both symmetrically and asymmetrically to regulate midgut homeostasis. Indeed, de Navascués et al. proposed that a neutral competition occurs between symmetrically dividing ISCs so that the newly formed daughter cells will adopt stochastically a stem or differentiated fate (de Navascués et al., 2012). Besides, it has recently been shown that ISCs have a cell-intrinsic polarity leading to the ISC asymmetric division. The polarization of ISCs results in the restriction of the Par complex (Bazooka, Par6 and the protein kinase aPKC) towards the apical cellular cortex of dividing ISCs (Goulas et al., 2012). The Par complex is involved in the positioning of the cleavage furrow along the apico-basal axis, which ensures different molecular composition of each daughter cell and thus their distinct destinies (Goulas et al., 2012). At the end of mitosis, the Par complex is subsequently dispatched to the apical daughter cell that will become the future EB (Goulas et al., 2012).

In *Drosophila* neuroblasts, it has been shown that the establishment of polarity by the Par complex and the orientation of the mitotic spindle during division trigger the asymmetric segregation of cell fate determinants between the two newly formed daughter cells (Lee et al., 2006). The neuroblast divides asymmetrically to generate one newly formed neuroblast and one ganglion mother cell (GMC). During neuroblast mitosis, aPKC phosphorylates the GMC differentiation factor Numb, which restricts Numb localization opposite to the Par crescent (Wirtz-Peitz et al., 2008; Atwood and Prehoda, 2009). Numb is also recruited at the basal cortical membrane of dividing neuroblasts through its binding with the protein Partner of Numb (Pon) (Lu et al., 1998; Wang et al., 2007). Numb is an inhibitor of Notch signalling, specifying binary cell fate during asymmetric division of the neuroblast (Spana and Doe, 1996). The daughter cell receiving Numb and Pon is thus depleted in Notch signalling activity.

In the adult *Drosophila* midgut, Notch signalling is also involved in the maintenance of the intestinal lineage (Ohlstein and Spradling, 2007; Bardin et al., 2010). The Delta ligand is present at the plasma membrane and within cytoplasmic vesicles in ISCs (Ohlstein and Spradling, 2007). The Notch receptor is expressed in both ISCs and EBs, but activation of Notch signalling is restricted to the EBs (Ohlstein and Spradling, 2007). Notch signalling regulates the proliferation of ISCs and is required to produce an appropriate fraction of ees versus ECs (Ohlstein and Spradling, 2007).

We have previously shown that internalized Delta ligands and Notch receptors traffic through a particular sub-population of early endosomes during the asymmetric division of the sensory organ precursor (SOP) cells (Bokel et al., 2006). These endocytic vesicles, called Sara endosomes, are characterized by the presence at their surface of the endosomal protein Sara (Smad Anchor for Receptor Activation) (Stenmark and Aasland, 1999; Itoh et al., 2002). Sara was discovered as an adaptor protein that mediates transforming

Department of Biochemistry, University of Geneva, 30 Quai Ernest-Ansermet, 1211 Geneva 4, Switzerland.

*Author for correspondence (marcos.gonzalez@unige.ch)

Received 27 September 2013; Accepted 17 March 2014

Development (2014) 141, 2014-2023 doi:10.1242/dev.104240

growth factor β (TGFβ) signal transduction in mammalian cells specifically (Tsukazaki et al., 1998). Bone morphogenetic protein (BMP), a member of the TGFβ superfamily, has recently been shown to play a negative role during ISC proliferation (Guo et al., 2013). Sara is not implicated in the transduction of BMP signals. Indeed, Sara binds specifically to unphosphorylated Smad2 and Smad3 transcription factors of the TGFβ complex, but not to the BMP-specific Smad1, Smad5 or Smad8 (Tsukazaki et al., 1998). We showed that Sara endosomes segregate asymmetrically during SOP mitosis (Coumailleau et al., 2009). This directional targeting of Sara endosomes containing Delta/Notch cargo biases Notch signalling between daughter cells and contributes to cell fate decision in the *Drosophila* SOP system (Coumailleau et al., 2009).

While Notch signalling is known to play a key role in the maintenance of intestinal lineage in the adult *Drosophila* midgut, the machinery controlling asymmetric Notch signalling during ISC mitosis still remains elusive. To study ISC mitosis, we established primary culture and time-lapse imaging conditions of the adult *Drosophila* midgut. Using this assay, we show (1) that ISCs do divide asymmetrically and (2) that Sara endosomes are partitioned asymmetrically. Sara endosomes are delivered to the EB daughter cell, opposite to a cortical Pon crescent inherited by the ISC. We also show that Notch signalling molecules traffic through Sara endosomes, thereby contributing to the enrichment of Notch signalling molecules in the presumptive EB daughter cell at work during the specification of the EB fate. Sara thus controls asymmetric intestinal cell fate assignation, which is implicated in adult *Drosophila* midgut homeostasis.

RESULTS

Sara endosomes are dispatched asymmetrically during ISC mitosis

In order to study the division of intestinal stem cells, we developed primary culture conditions to perform live imaging of the adult *Drosophila* midgut (for details see Materials and Methods). To establish primary culture and imaging conditions, we first infected flies with the gram-negative bacteria *Erwinia carotovora carotovora* (*Ecc15*), which increased the number of dividing ISCs significantly (see supplementary material Fig. S1A). Once the conditions were established, *Ecc15* infection was removed from the protocol. On average, in non-infection conditions, we observed around 3±3 dividing ISCs per midgut, which we imaged by spinning disc microscopy.

To study the segregation of Sara endosomes in dividing ISCs, we imaged Sara-GFP driven by *esg-Gal4* combined with *tub-Gal80^{ts}* (Buchon et al., 2009). In prophase, ISCs contain an average of 22±2 (n=13 fixed cells) Sara endosomes per cell (Fig. 1A). These endosomes fuse during mitosis, resulting in a lower number of larger vesicles (Fig. 1C,D). Fig. 1B-D show that, during anaphase, these Sara vesicles are targeted to the cleavage plane and are subsequently preferentially dispatched to one of the daughter cells at cytokinesis (supplementary material Movies 1, 2). At early cytokinesis, Sara endosomes are enriched by a factor of three in one of the daughters: on average 75±2% (n=28 cells) of the Sara endosomes are targeted to one of the daughters. The asymmetry can also be observed if the volume of endosomes is considered: 76±3% (n=28 cells) of the Sara endosome volume is targeted to one of the cells.

The asymmetric behaviour of Sara endosomes is not universal for all compartments in the endosomal pathway. In particular, recycling endosomes and late endosomes, which are labelled by Rab11 and Rab7, respectively, are dispatched more symmetrically during ISC mitosis (supplementary material Fig. S1B,C and Movie 3). These observations are reminiscent of the behaviour of Sara endosomes and other endosomal compartments in different asymmetric division models, such as the sensory organ precursors (SOPs) and larval neuroblasts (Coumailleau et al., 2009). In the case of the SOPs, Sara endosomes are specifically enriched in the pIIa cell by a factor of 85% (Coumailleau et al., 2009).

Sara endosomes are dispatched to the enteroblast after cytokinesis

It has recently been proposed that, as in the SOP and the neuroblast, ISC asymmetric division is controlled by the Par complex (Goulas et al., 2012). The Par complex triggers the asymmetric localization of cortical factors, including Numb, into the signal-sending cell: the pIIb in the SOP lineage (Roegiers et al., 2001) and the self-renewed ISC in the adult midgut (GFP-Numb) (Goulas et al., 2012). Consistently, it was shown that the Par complex forms a cortical crescent in the ISC, in a region that forecasts the future EB daughter cell (Goulas et al., 2012). In addition, downstream of the Par complex, Numb can be phosphorylated by aPKC, which indeed causes Numb-GFP to be excluded from the Par crescent and to be restricted to the newly formed ISC (Goulas et al., 2012).

In order to study the asymmetric dispatch of the Pon cortical factor during ISC mitosis, we performed live imaging of an RFP fusion to the cortical localization domain (LD) of the Numb-binding protein Pon (Partner of Numb) (Perdigoto et al., 2008; Coumailleau et al., 2009). In the SOP, Pon^{LD}-RFP colocalizes with Numb in the anterior cortex, which will contribute to the specification of the pIIb daughter cell (Mayer et al., 2005). Fig. 2 shows that, during metaphase, Pon^{LD}-RFP forms a crescent at the cortex of the dividing ISC. The cortical pool of Pon is then specifically inherited by one of the daughters (Fig. 2; see supplementary material Movie 4). Because of the relationship between Pon and Numb, this strongly suggests that the cell inheriting Pon corresponds to the one that will adopt the ISC fate (Goulas et al., 2012). Indeed, these results are consistent with the asymmetric targeting into the EB of the Par-complex proteins that, in turn, by aPKC-dependent phosphorylation, excludes Numb-GFP from the EB and restricts it to the ISC (Goulas et al., 2012). Therefore, as Pon is a partner of Numb, our data suggest that Pon is inherited by the future ISC.

Fig. 2 also shows that Sara endosomes are asymmetrically targeted to the Pon^{LD}-RFP-negative cell (supplementary material Movie 4). Therefore, Sara endosomes are dispatched into the future EB. This indicates that, as in the SOP, Sara endosomes are inherited by the signal-receiving cell, which activates Notch signalling. This raises the question of whether the ligand Delta and its receptor Notch traffic through Sara endosomes.

Delta and Notch traffic through Sara endosomes

During prophase/metaphase, both Notch and Delta traffic through Sara endosomes (Fig. 3A-C): 74±3% (n=17 cells) of Sara endosomes contain Delta cargo similar to the SOP system (Coumailleau et al., 2009). In dividing ISCs, both Delta and Notch are seen in Sara endosomes targeted into the presumptive EB (Fig. 3D,E). During cytokinesis, these pools of Notch and Delta are dispatched asymmetrically (Fig. 3D,E), akin to what was observed for Sara endosomes (Fig. 1B,C and Fig. 2). These results indicate that, as in the SOP, both the ligand and its receptor move to the Notch signal receiving cell during ISC asymmetric division.

Ohlstein et al. observed that, in dividing ISCs, Delta-positive vesicles are homogeneously distributed in anaphase (Ohlstein and Spradling, 2007). Later, Delta accumulates in interphase ISCs (Ohlstein and Spradling, 2007). Based on this observation, they argue that Delta segregates randomly between daughter cells during ISC mitosis and is then downregulated in the post-mitotic EB. This

Development (2014) 141, 2014-2023 doi:10.1242/dev.104240

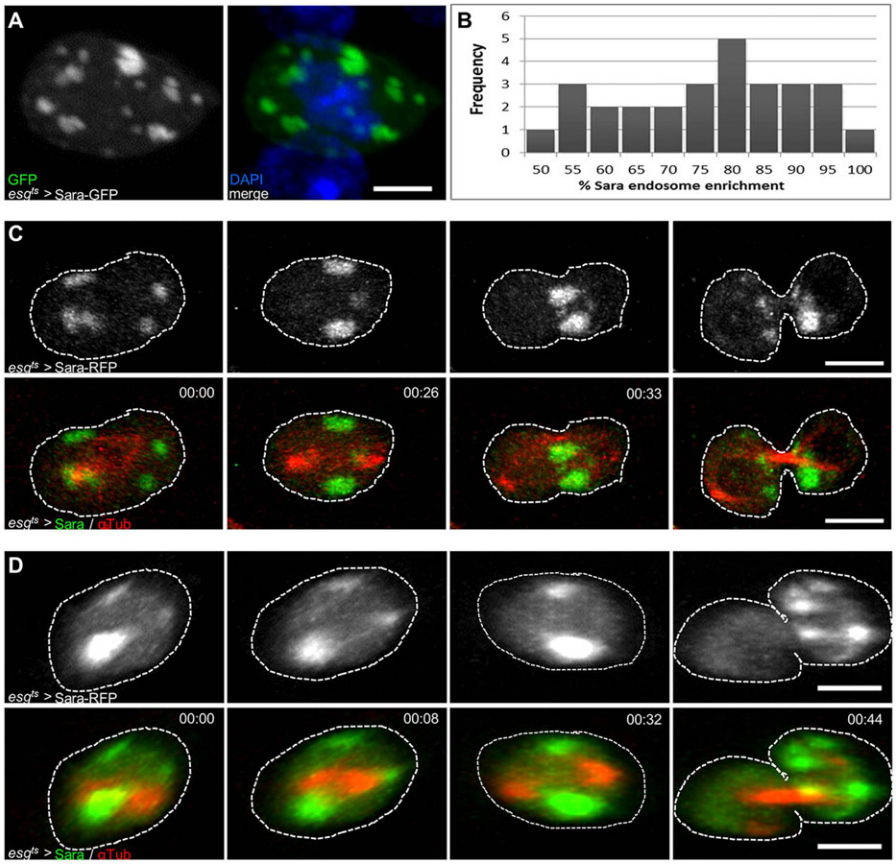

Fig. 1. ISCs divide asymmetrically and Sara endosomes are unequally partitioned during ISC division in the adult *Drosophila* midgut. (A) Analysis of the number of Sara-GFP endosomes present in dividing ISC at prophase. Sara endosomes are detected GFP immunostaining in fixed cells (n=13 cells). Scale bar: 3 µm. (B) Frequency distribution of Sara endosome enrichment from time lapse of dividing ISCs in cytokinesis (n=28 cells). (C,D) Time-lapse images showing the asymmetric dispatch of Sara endosomes during ISC mitosis. (C) Z-projection snapshots from a movie showing a dividing ISC expressing *UAS-Sara-RFP* (green) and *UAS-α-Tubulin-GFP* (red) driven by *esg-Gal4* combined with *tub-Gal80*^{ts} (*esg*^{ts}) observed 11 h after oral infection by *Ecc15*. (For a representative movie from a data set of n=5 cells, see supplementary material Fig. S1 and Movie 1.) (D) During ISC mitosis, Sara endosomes segregate asymmetrically in one of the two daughter cells. [For a representative movie from a data set of n=17 cells (no *Ecc15* infection), see supplementary material Movie 2.] Dashed line indicates cell outline by monitoring the cytosolic pool of Sara in over-contrasted images (not shown). Scale bars: 5 µm.

assumes that the random distribution they observed in anaphase reflects the situation later, at cytokinesis and abscission. Instead, we found that in early cytokinesis (where staging was assessed by monitoring the midbody), internalized Notch and Delta colocalize with Sara endosomes and are asymmetrically dispatched into the future EB (Fig. 3D,E).

We also observed that shortly after division, this cohort of Delta/Notch molecules coming from the ISC and trafficking through Sara endosomes is degraded in the EB: Delta accumulates only in steady-state interphase ISCs and is absent in post-mitotic EBs (Fig. 3F). One reason for this could be that Delta is short-lived in newly formed EBs. To address this point, we slowed down lysosomal degradation using chloroquine treatment. This caused an accumulation of Delta that is seen at higher levels in ISCs (supplementary material Fig. S2A,B). In addition, we observed an accumulation of Delta in EBs that allow us to capture the Delta pool inherited from the ISC (supplementary material Fig. S2C,D). This pool is normally transient and quickly cleared after division. Therefore, Delta is actively degraded in the EB and resynthesized in the ISC after mitosis. These observations are consistent with previous reports where Delta accumulation is used as marker for the ISC (Ohlstein and Spradling, 2007). As Delta/Notch traffic asymmetrically through Sara endosomes during ISC mitosis, this raises the possibility that Sara itself plays a role in the regulation of Notch signalling activity and, thus, in ISC self-renewal and EB differentiation.

Sara mutants phenocopy Notch loss of function in the midgut

To determine the role of Sara in the adult *Drosophila* midgut, we looked at *Sara* mutant flies. *Sara* loss of function leads to semi-lethality: only 5% of *Sara*^{12}/*Sara*^{12} animals survive to adulthood. Lethality can be largely rescued by the expression of Sara-GFP driven by the Ubiquitin promoter: 77% survival of *Sara*^{12}/*Df(2R)48, Sara*$^{-}$ flies containing two copies of *Ubi:Sara-GFP*.

The surviving *Sara*$^{-}$ mutants do show a midgut phenotype at 15 days after hatching (Fig. 4A,B). The midgut length is significantly reduced in *Sara*^{12}/*Sara*^{12} and *Sara*^{12}/*Df(2R)48*, *Sara*$^{-}$ mutants with respect to wild type (Fig. 4B). The mitotic index is also significantly decreased by half in absence of Sara (Fig. 4C), indicating a proliferation defect. These observations reveal that Sara plays an essential role during adult *Drosophila* midgut homeostasis.

We then studied whether deletion of Sara affects the ISC compartment in the adult midgut. In *Sara* mutants, the number of ISCs in the posterior midgut (most posterior 230 µm region adjacent to the pylorus) 15 days after hatching is significantly increased compared with wild type (Fig. 4D,E). Similar results were obtained using Sara RNA interference (RNAi) (supplementary material Fig. S3A-B′). This phenotype resembles the effects of loss of Notch signalling in the adult midgut (Ohlstein and Spradling, 2006, 2007), which uncovered a role for Notch signalling during asymmetric cell fate assignation and ISC self-renewal. Furthermore, epistasis experiments show that Notch signalling acts downstream Sara function, as expression of an activated form of Notch, together with Sara RNAi results in a Notch gain-of-function phenotype (decreased number of ISCs) (supplementary material Fig. S3C-D′). These results are therefore consistent with a scenario where asymmetric dispatch of Sara endosomes during ISC mitosis plays a role in cell fate assignation mediated by Notch signalling.

Sara contributes to asymmetric cell fate assignation in the ISC lineage

To explore the Notch-dependent function of Sara in cell fate determination, we generated *Sara*^{12} homozygous mutant MARCM

Development (2014) 141, 2014-2023 doi:10.1242/dev.104240

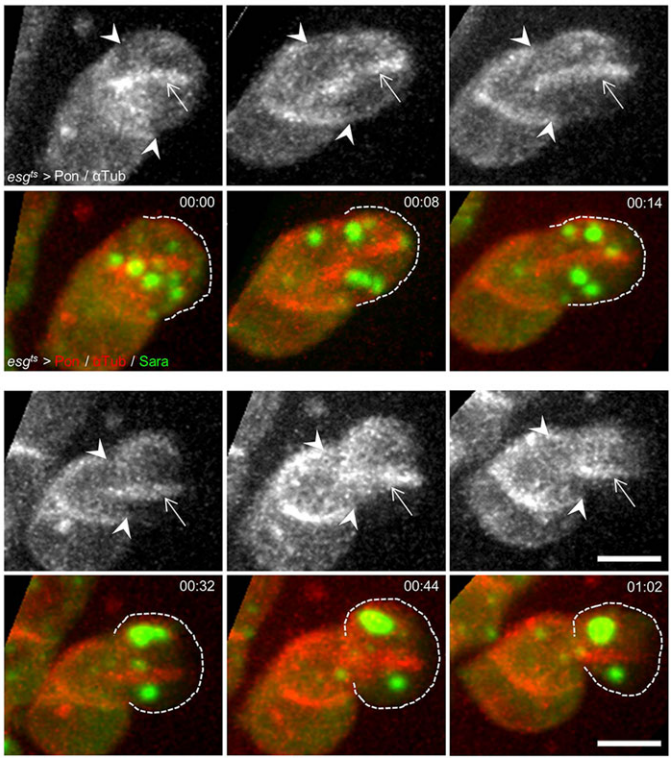

Fig. 2. Asymmetric dispatch of cortical Pon and Sara endosomes during ISC mitosis. Z-projection images from a movie showing a dividing ISC expressing *UAS-Pon-RFP* (flanked by two arrowheads), *UAS-mCherry-α-Tubulin* (arrow; both white; red in merge) and *UAS-Sara-GFP* endosomes (green) under the control of *esg-Gal4* combined with *tub-Gal80^{ts}*. Pon crescent is asymmetrically inherited by the newly formed ISC, opposite to its sibling receiving Sara endosomes (*n*=4 cells). Scale bars: 5 µm (see supplementary material Movie 4).

clones and looked at the cell identities in the intestinal lineage 10 days after clone induction. We studied the activation of Notch signalling by using a previously established Su(H)-lacZ Notch reporter (Furriols and Bray, 2001). The proportion of multiple cell clones containing at least one Su(H)-positive cell in absence of Sara (50.6%; *n*=85 clones) is substantially reduced compared with wild type (67.3%; *n*=171), suggesting a role of Sara during Notch signalling.

We also noticed that *Sara* loss of function affects cell viability: the number of *Sara* mutant clones recovered is significantly lower than the one in wild-type condition (Fig. 5A,B). Moreover, *Sara* mutation leads to a decrease in the effective proliferation rate, which is reflected in a reduced number of cells per clone (Fig. 5C-E). We estimated that in *Sara*$^{-}$ mutant clones, the ISC cell cycle length is prolonged up to seven-fold (for estimation of the relative cell cycle length see Materials and Methods). This is consistent with the reduced size of *Sara*$^{-}$ mutant midguts (Fig. 4A).

To study specifically whether Sara is important for asymmetric cell fate assignation during ISC mitosis, we analysed clones composed of only two cells (doublets) and determined the ISC identity of the two cells by Delta immunostaining (Fig. 5C′,D′,F). We chose to restrict our analysis to doublets because larger clones may also arise from fusion of two or more independent clones. In addition, clones were induced 5 days after hatching to ensure that the founder of the clone is not a precursor of ISC (pISC), which are known to divide symmetrically shortly after eclosion (O'Brien et al., 2011; Takashima et al., 2011).

In the posterior-most region of the midgut, wild-type doublets containing two Delta-positive ISCs are rare (1%; *n*=101 doublets) (Fig. 5F), as previously reported (Perdigoto et al., 2011). The presence of pISCs in clones induced earlier (1 to 3 days) explains the higher frequency of doublets composed by two Delta-positive cells obtained in previous reports (Goulas et al., 2012). In *Sara*^{12}/*Sara*^{12} doublets, the frequency of symmetric divisions leading to two Delta-positive cells is increased by 10-fold (*n*=53 doublets) (Fig. 5F), indicating that Sara plays a role in the asymmetric cell fate assignation during mitosis, which gives rise to one ISC and one EB. This could be due to a symmetric segregation of Delta molecules during mitosis in the absence of Sara. Indeed, we observed symmetric dispatch of internalized Delta at cytokinesis (supplementary material Fig. S5A). These results indicate that Sara endosomes are responsible for the asymmetric inheritance of Delta during ISC mitosis and that Sara itself thus contributes to Notch-dependent asymmetric cell fate assignation.

We also noticed a significant depletion of the number of *Sara*^{12} mutant doublets with a single Delta-positive cell (supplementary material Fig. S4B). Although this depletion can also suggest a decrease of asymmetric divisions in absence of Sara (symmetric division giving rise to two ISCs or differentiated cells), we cannot exclude that this is due instead to apoptosis events eliminating the Delta-positive cell in the lineage.

It is worth noting, that the frequency of symmetric ISC divisions in wild type is higher than the 1% observed in our control doublets. This is because we are chasing these doublets under very stringent conditions: 10 days after clone induction, when many of the clones did divide to generate lineages of more than only two cells. Previous reports have estimated that around 40% of the divisions are symmetrical (O'Brien et al., 2011). Our analysis of multiple cell clones is consistent with this frequency (supplementary material Fig. S4A). This is also compatible with our time-lapse analysis of Sara endosome segregation during ISC division: we find around 30% of the cells segregating Sara endosomes in a quasi-symmetrical fashion (Fig. 1B). In summary, when ISC division is asymmetric, Sara endosomes are responsible for the directional segregation of the Delta ligand and contributes to the specification of different cell fates.

Sara promotes the EC fate

Notch signalling is involved both in asymmetric cell fate assignation during ISC division and, later, in the specification of EB: the differentiating EB will preferentially become an enterocyte (EC) instead of an enteroendocrine cell (ee) (Ohlstein and Spradling, 2007). Consistent with the role of Notch signalling in EB differentiation into an EC versus an ee, the number of ees is increased at the expense of the EC compartment in *Sara*^{12} mutant clones (Fig. 5G). Thus, 10 days after MARCM induction, the ratio ee/EC in multiple cell clones is increased from 0.4 in wild-type clones (*n*=46) to 0.9 in *Sara*^{12} mutant clones (*n*=19). These observations suggest that Sara plays a cell-autonomous role during Notch signalling both during cell fate determination in dividing ISCs and, later, during the specification of the EB fate.

Sara overexpression triggers symmetric ISC divisions

Consistent with a role for the asymmetric distribution of Sara endosomes and the Notch/Delta cargo therein in asymmetric cell fate assignation, overexpression of Sara in clones also affects the fate of ISC daughter cells. Sara overexpression is not detrimental to cell viability (Fig. 6A,B) or proliferation rate (Fig. 6C-E), in contrast to Sara loss of function. Therefore, large clones containing several Delta-positive ISCs can be observed (Fig. 6D). Indeed, in cell

Development (2014) 141, 2014-2023 doi:10.1242/dev.104240

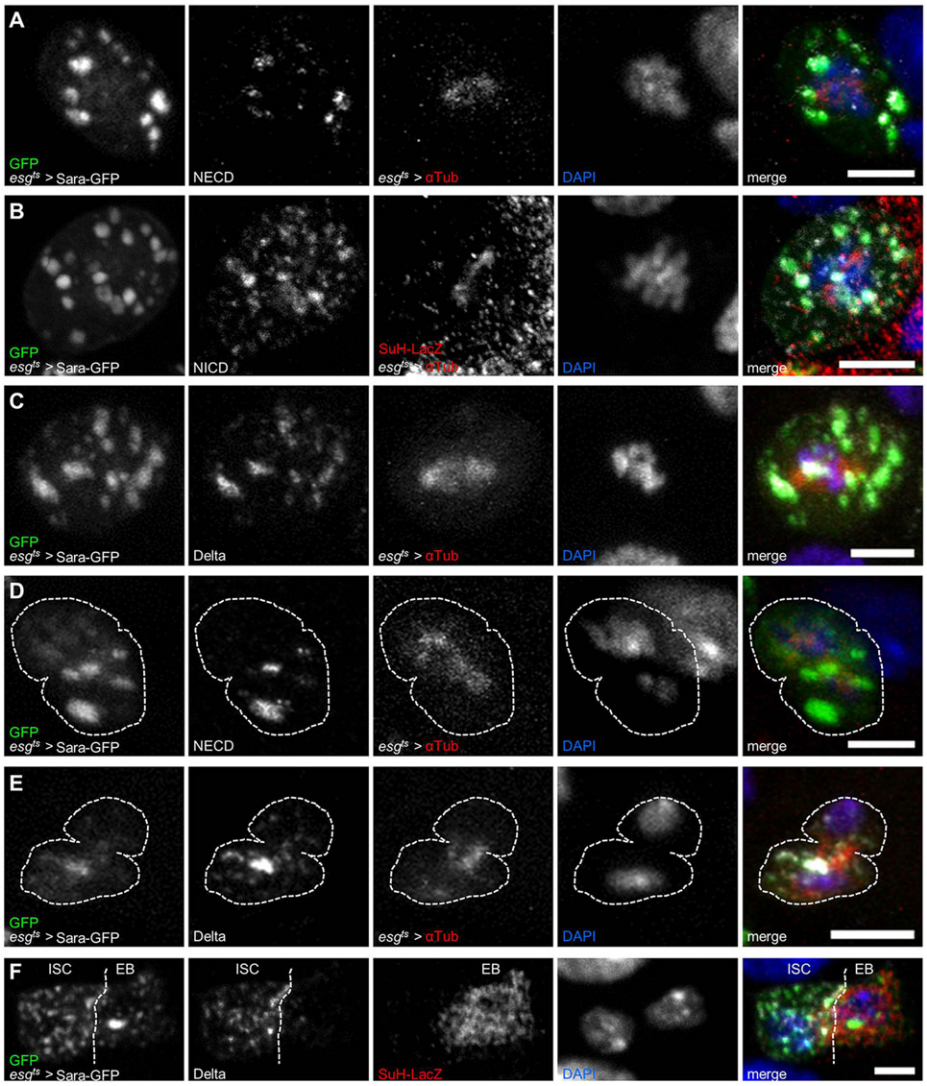

Fig. 3. Internalized Notch and Delta traffic through Sara endosomes in the future EB. (A-E) Expression of *UAS-Sara-GFP* and *UAS-mCherry-α-Tubulin* using the *esg*^{ts} system. Sara endosomes are detected by GFP immunostaining. Scale bars: 5 µm. (A-C) Z-projection confocal images of dividing ISCs at prophase. Immunostaining for extracellular (A, NECD, white in the merge, *n*=9 cells) and intracellular domains (B, NICD, white, *n*=18 cells) of Notch, and for Delta (C, white, *n*=17 cells), showing the pool internalized into Sara endosomes (green in the merge). (D,E) Z-projection confocal images of dividing ISCs at early cytokinesis. The presence of the midbody labelled by *mCherry-α-Tubulin* (red in merge) indicates the mitotic stage. Only one focal plane is shown for DAPI staining in D due to an overlap with surrounding nuclei. (D) The Notch receptor is asymmetrically delivered in the daughter cell inheriting Sara endosomes (97.72% in this cell). (E) Similar results were obtained for Delta (96.02% in this cell). Dashed line indicates cell outline. (F) At interphase, Sara endosomes (green in merge) are present in both ISC and EB. EBs are identified by the expression of Su(H)-LacZ Notch reporter and detected by immunostaining against β-Galactosidase (red in merge). Delta ligand is restricted to the ISC after division, as previously reported (*n*=16 cells) (Ohlstein and Spradling, 2007). Scale bars: 3 µm.

clones overexpressing Sara, the frequency of lineages containing two or more Delta-expressing ISCs is increased by fourfold (*n*=47) in comparison with control flip-out clones (*n*=21) (Fig. 6F). These results are consistent with a scenario where Sara overexpression oversaturates the machinery that mediates the asymmetric inheritance of Sara endosomes and thus of internalized Notch/Delta proteins. To study the segregation of Notch signalling molecules in Sara overexpressing ISCs during mitosis, we performed immunostaining of the extracellular domain of Notch and Delta (supplementary material Fig. S5B,C). Both Notch and Delta are more symmetrically dispatched at cytokinesis than in wild type (Fig. 3D,E), indicating that ISCs divide symmetrically when Sara is overexpressed.

This suggests a scenario, similar to the SOP, where the decision to become pIIa (Notch^{+} cell) versus pIIb (Notch^{-} cell) is mediated by a mechanism of mutual inhibition. In the SOP, the switch to maintain Notch signalling is decided on the basis of the comparative, relative levels of Notch signalling in the two sibling cells.

DISCUSSION

During physiology of adult *Drosophila* midgut, stem cell self-renewal is essential to maintain a pool of dividing cells, which compensates the death of differentiated cells. In this report, we showed that ISCs can divide asymmetrically to generate one daughter, which remains a stem cell, whereas the other differentiates into an enterocyte or enteroendocrine cell. During ISC mitosis, Notch/Delta contained within Sara endosomes are directionally dispatched to be inherited by the newly formed EB. These Sara endosomes and their cargo contribute themselves to the generation of asymmetric lineages within the midgut posterior-most region. This conclusion is based on the following five key observations: (1) the asymmetric cortical localization of Pon during ISC mitosis, which is inherited by the newly formed ISC daughter (Fig. 2); (2) the asymmetric segregation of Sara endosomes away from the Pon marker in cytokinesis, thereby accumulating into the presumptive EB (Fig. 2); (3) the trafficking of both Notch and Delta through Sara endosomes and their asymmetric partitioning during ISC mitosis (Fig. 3); (4) the expansion of the ISC compartment in *Sara* mutants (Fig. 4B,C); and (5) the increase of symmetric lineages composed of two Delta-positive cells, both in *Sara* mutant and Sara overexpression clones (Figs 5, 6), which is similar to Notch loss-of-function phenotype (Ohlstein and Spradling, 2007).

Our results are therefore consistent with a scenario where Notch/Delta molecules that are endocytosed in the ISC traffic through Sara endosomes. These Sara endosomes go to the central spindle and are finally targeted to the presumptive EB. Carrying Notch and Delta, the EB initiates its fate decision with the activation of Notch signalling and thereby becomes the signal-receiving cell. This

Development (2014) 141, 2014-2023 doi:10.1242/dev.104240

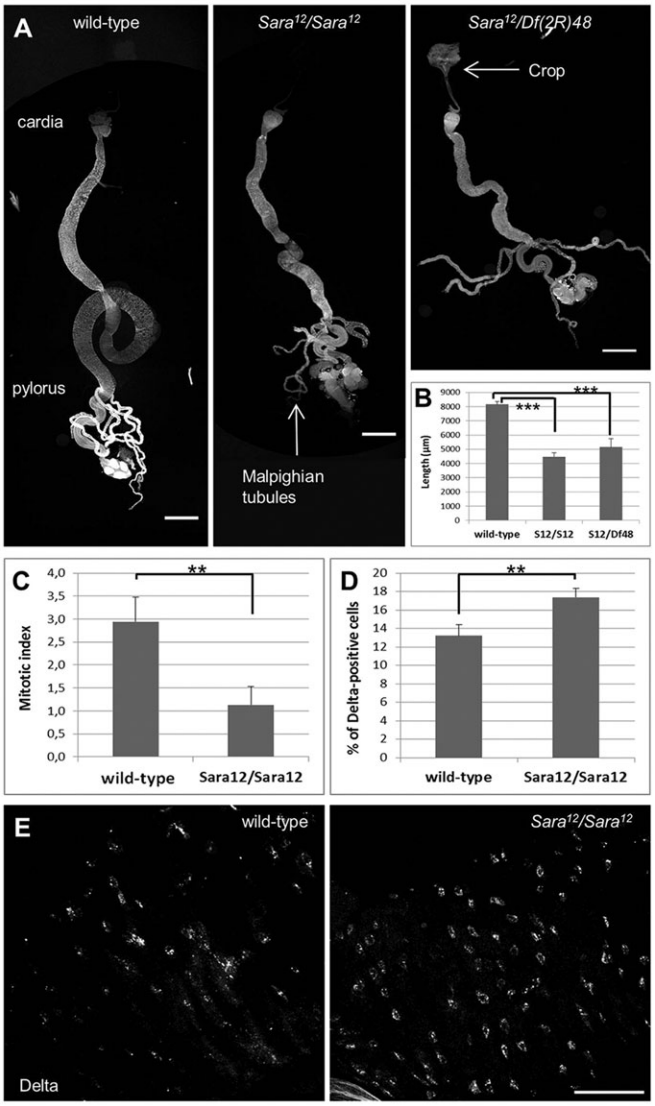

Fig. 4. Sara mutation leads to an expansion of the Delta-positive cell compartment coupled with a reduction of the mitotic index. (A) Z-projection confocal images revealing the morphology of a 15-day-old wild-type adult *Drosophila* midgut (DAPI staining, n=16 guts), $Sara^{12}/Sara^{12}$ (n=11 guts) and $Sara^{12}/Df(2R)48$ (n=6 guts) mutants. At the anterior part of the gastrointestinal tract, the cardia marks the limit between the crop and the midgut, whereas at the posterior part the pylorus delimits the midgut from the hindgut. Malpighian tubules are present close to the pylorus. Scale bars: 500 µm. (B) Length of adult midguts 15 days after hatching. Sara mutant midguts are significantly shorter compared with wild type (***P<0.001; one-way analysis of variance). (C) Mitotic index [(number of PH3-positive cells/number of Delta-positive cells in the posterior region)×100] in wild-type (n=7 guts) and $Sara^{12}/Sara^{12}$ mutants (n=4 guts). Difference is statistically significant (**P=0.042; Student's t-test). (D) Proportion of ISCs relative to the total number of cells in the posterior midgut in wild-type (n=11 guts) and $Sara^{12}/Sara^{12}$ (n=6 guts), 15 days after hatching. Difference is statistically significant (**P=0.036; Student's t-test). Error bars indicate s.e.m. (E) Z-projection confocal images of Delta-positive cells in the adult *Drosophila* posterior midgut 15 days after hatching. Delta-positive cell number is increased in absence of Sara. Scale bar: 50 µm.

mechanism might be conserved in vertebrates. Indeed, it has recently been shown that the mammalian homologue of Delta, Dll1, is asymmetrically inherited during mitosis of mouse neural stem cells, in a mechanism that has been implicated in maintaining stem cell quiescence (Kawaguchi et al., 2013).

Sara endosome asymmetry and the model of neutral competition

Our live imaging of Sara endosomes showed frequent asymmetric inheritance of these endosomes during ISC divisions (Fig. 1B-D, Fig. 2): indeed, on average, 75% of the Sara endosomes are asymmetrically targeted into one of the two daughter cells (Fig. 1). This is consistent with our clonal analysis of the midgut lineages and similar previous reports showing that, although symmetric division can also take place in the midgut, the asymmetric lineages are the most frequent ones (O'Brien et al., 2011; Goulas et al., 2012).

It has recently been shown that homeostasis in the mammalian intestine can also be achieved by a mechanism implicating ISC symmetric division and neutral clonal competition in the ISC compartment (Snippert et al., 2010). A similar mechanism of self-renewal has been proposed in the *Drosophila* adult midgut (de Navascués et al., 2012). In this scenario, dividing ISC cells can give rise to two ISCs, two EBs, or one ISC and one EB. They proposed that ISCs divide symmetrically, and the fate of the progeny is resolved through lateral inhibition mediated by Dl/N signalling (de Navascués et al., 2012). They speculate that asymmetric cell fate determination occurs by lateral inhibition within the lineage and therefore only one daughter cell is selected for the ISC fate. Conversely, symmetric cell fate determination would happen only when competition happens between two different lineages, so that one sibling pair become ISCs and the other sibling pair become EBs (de Navascués et al., 2012). They acknowledge that, alternatively, their data cannot exclude the possibility that an intrinsic mechanism operating in a single lineage determines stochastically whether the division is symmetric or asymmetric (de Navascués et al., 2012). In this report, we show that segregation of Sara/Delta endosomes is consistent with such alternative intrinsic mechanism, whereby asymmetry of Sara would bias divisions to be asymmetric, while more symmetric segregation of these endosomes (the left tail in Fig. 1B) could allow divisions to be symmetric.

ISC versus ISC-like in the posterior midgut

$Sara^{-}$ mutants produce more Delta-positive cells, but the proliferation rate of these cells is affected (Fig. 4C). Moreover, mutation in Sara causes symmetric ISC divisions [two Delta-positive cells are generated (Fig. 5D,F)], but this does not lead to an increase in clone size (Fig. 5E). As their proliferative capability is impaired, it might be more precise to call these cells 'ISC-like' cells. By contrast, in Sara overexpression conditions, the proliferative capability of the supernumerary ISCs are intact, leading to an increased of clone size (Fig. 6E).

Nevertheless, both Sara mutation and overexpression lead to symmetric generation of two Delta-positive cells. These results imply that it is the comparative levels of Notch signals (the cargo of Sara endosomes) between the two daughters that is instructive to the binary fate choice between EB and ISC. Such a process is consistent with the notion that Notch signalling in this cell pair is mediated by 'mutual inhibition' [each of the cells tries to inhibit its neighbour (de Navascués et al., 2012)] akin to the mechanism in place during the singling out of SOPs from proneural clusters (reviewed by Fürthauer and González-Gaitán, 2009b).

MATERIALS AND METHODS

Drosophila stocks

Drosophila stocks were maintained at 18-21°C on standard fly medium, which was complemented with dry yeast and changed every 2-3 days during the experimental period. Adult midguts were examined at the time points

Development (2014) 141, 2014-2023 doi:10.1242/dev.104240

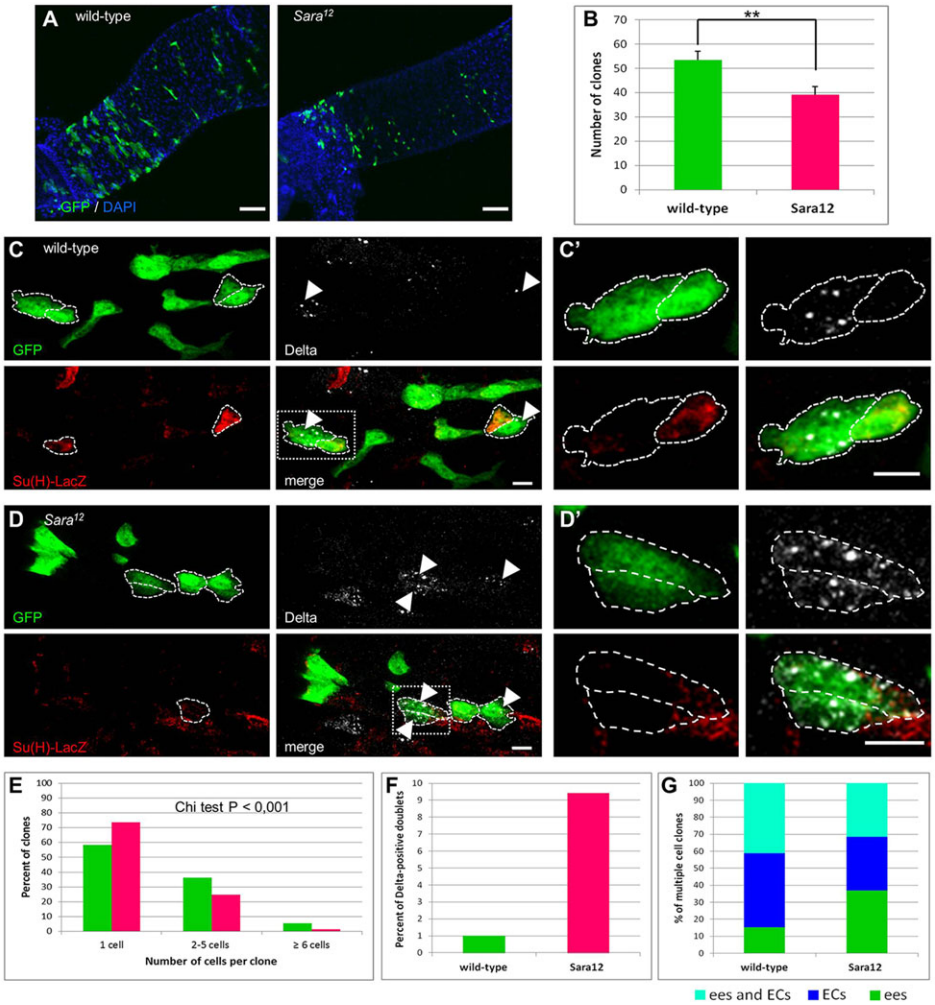

Fig. 5. Sara contributes to the asymmetric division of ISCs. (A) Z-projection confocal images of GFP-positive wild-type and *Sara*^{12} homozygous mutant MARCM clones (green) in the adult posterior midgut 10 days after clone induction. Scale bars: 50 µm. (B) Reduced number of *Sara* mutant clones in posterior midguts (wild type, *n*=1228 clones, *n*=23 guts versus *Sara*^{12}, *n*=976, *n*=25). Difference is statistically significant (***P*=0.007; Student's *t*-test). Error bars indicate s.e.m. (C,D) *Sara* mutant clonal analysis. ISCs and 'ISC-like' cells were detected by a Delta staining (white, arrowheads). Enteroblasts were identified by Su(H)-LacZ Notch reporter expression (red). Dashed boxes in C and D indicate the regions showed at higher magnification in C′ and D′. (C′) Wild-type clone composed of one Delta-positive ISC and one EB corresponding to an asymmetric division of an ISC. (D′) *Sara* mutant clone composed of two Delta-positive cells corresponding to a symmetric division of the mother ISC. Scale bars: 5 µm. (E) ISC proliferation rate is reduced in absence of Sara. Frequency distribution of the number of cells per clone. Data are given as the percentage of the total number of clones (wild type, *n*=1228 clones versus *Sara*^{12}, *n*=976). The size distribution of MARCM clones is significantly perturbed upon Sara loss of function (*P*<0.001; Chi-square test). (F) Quantification of the proportion of doublets, composed of two Delta-positive cells, relative to the total number of doublets (wild type, *n*=101 doublets versus *Sara*^{12}, *n*=53). (G) Proportion of multiple cell clones composed of only ees (green), ECs (blue) or both differentiated cell types (turquoise) relative to the total number of multiple cell clones (wild type, *n*=46 multiple cell clones versus *Sara*^{12}, *n*=19). Sara mutation promotes ee cell fate assignation and phenocopies Notch loss of function.

indicated in each figure. Only females were analysed in this study because of the high nutritional demand for egg production. Fly strains used were:

OregonR (wild type)
w; esg-Gal4,tub-GAL80ts/CyO; pUAST-mCherry-α-Tubulin84B(2M)/TM6B (C. Seum, University of Geneva, Geneva, Switzerland)
w; UAS-Sara-GFP
w; UAS-Rab11-GFP(C1)
w; UAS-Rab7-GFP(B1)/TM3,Sb
w; UAS-Pon-RFP; UAS-Sara-GFP/TM6B
w; esg-Gal4/Cyo,act-GFP; tubulin-Gal80ts/MKRS (gift from N. Buchon, EPFL, Lausanne, Switzerland)
Sara12 (Bokel et al., 2006)
w; Sara12(1B)/CyO,actGFP
w; Sara12(H2)/Cyo; Dl-Gal4,Tubulin-Gal80ts/pUAST-mCherry-α-Tubulin84B
Df(2R)48 (Johnson et al., 2004)
w; If/CyO,actGFP; TM6B/MKRS
Su(H)GBE-lacZ (Furriols and Bray, 2001)
Su(H)GBE-lacZ; Sara12(1B)/CyO,actGFP; Ubi:Sara-GFP(15.2)/TM6B
w; Ubi:Sara-GFP(8.3)/SM6
P[hsFLP]12,y^{1}*w; nocSco/CyO* (1929 Bloomington stock)
w; CyO,actGFP/P[FRT(whs)]G13; MKRS/TM6B
Su(H)GBE-lacZ; P[FRT(whs)]G13,P{tubP-Gal80}/CyO,actGFP; P{TubP-Gal4},P{UAS-GFP}/TM6B
y^{1}*w,Act>CD2>Gal4; UAS-GFP*
w; UAS-HM-Sara/TM3,Sb (Bennett and Alphey, 2002)
w; esg-Gal4,UAS-src-GFP,tubulin-Gal80ts
w^{1118}*; P{GD8765}v19150/Cyo* (Sara RNAi, VDRC)
w; If/Cyo^{wz}*; UAS-Notch*^{cdc10} [a truncated active form of the intracellular domain of Notch (NICD)] (Brennan et al., 1999).

Information on *Drosophila* genes and stocks is available on the FlyBase website (http://flybase.bio.indiana.edu).

Development (2014) 141, 2014-2023 doi:10.1242/dev.104240

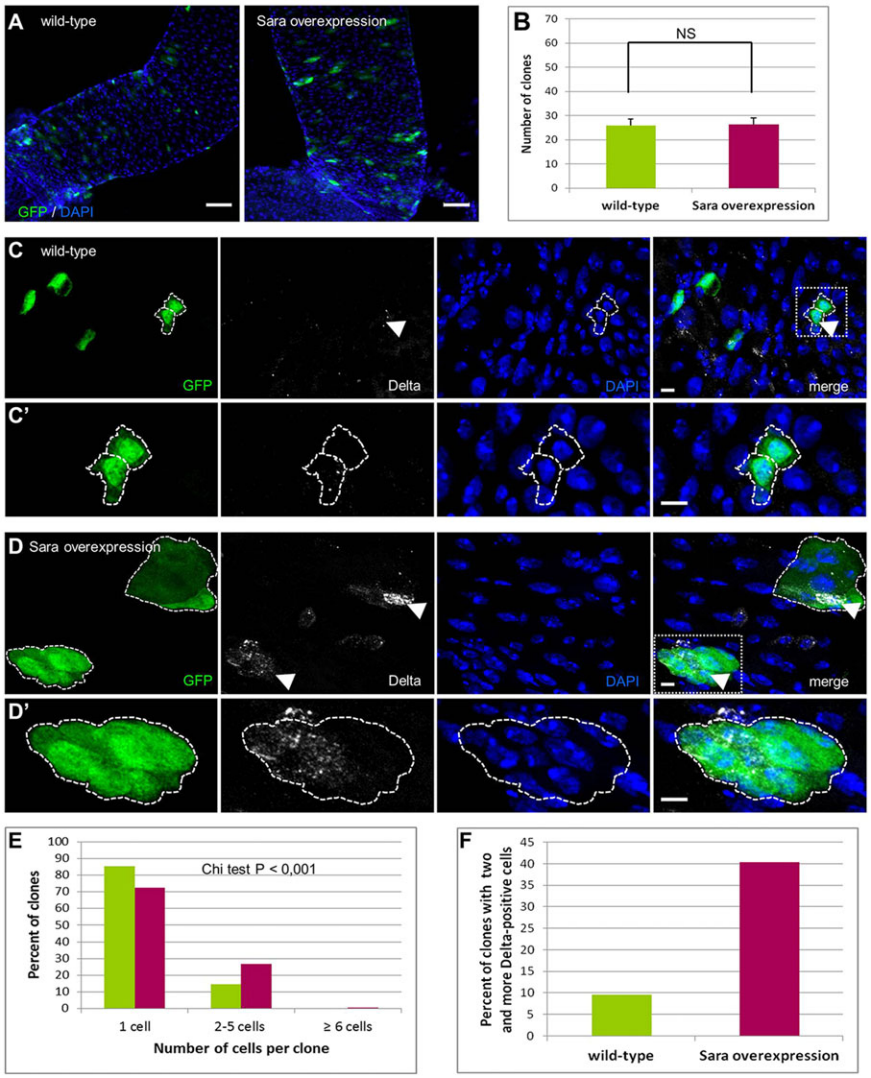

Fig. 6. Sara overexpression induces symmetric cell fate decision during ISC mitosis. (A,C,D) Z-projection confocal images of adult posterior midguts labelled with DAPI (blue) and containing either control or Sara-overexpressing flip-out clones marked by GFP (green), 10 days after induction. Scale bars: 50 µm in A; 5 µm in C,D. (B) Average flip-out clone frequency in posterior midguts is similar in wild-type and Sara overexpression conditions (no statistical difference; Student's *t*-test). Error bars indicate s.e.m. (C,D) Higher magnification of the flip-out clones as shown in A. There are more cells per clone in Sara overexpression conditions when compared with control. The number of cells per flip-out clones (green) is determined by monitoring the nuclei labelled by DAPI (blue). Dashed boxes in C,D indicate the regions shown at higher magnification in C′ and D′. Sara overexpression (D′) leads to an increase in the number of Delta-positive cells (white, arrowheads). We also noticed an increased level of Delta expression in Sara-overexpressing clones, suggesting a potential effect of Sara overexpression in endosomal maturation. Dashed lines indicates clone/cell outlines. (E) Frequency distribution of flip-out clone sizes. Sara overexpression significantly affects the size distribution of flip-out clones ($P<0.001$; Chi-square test). (F) Frequency of clones containing at least two Delta-positive cells relative to the total number of multiple cell clones (wild type, $n=21$ multiple cell clones versus Sara overexpression, $n=47$). For genotypes, see Materials and Methods.

Mosaic analysis

Crosses and progeny were kept at 18°C. The mosaic analysis with repressible cell marker (MARCM) technique (Lee and Luo, 1999) was used to induce somatic recombination and generate either wild-type MARCM clones (*y*^{1}*w P*[*hsFLP*]*12/Su(H)Gbe;P*[*FRT(whs)*]*G13/P*[*FRT(whs)*]*G13,P*[*tubP-GAL80*]*; P*[*TubP-GAL4*]*,P*[*UAS-GFP*]*/+*) or *Sara* homozygous mutant MARCM clones (*y*^{1}*w P*[*hsFLP*]*12/Su(H)Gbe;P*[*FRT(whs)*]*G13Sara12/P*[*FRT(whs)*]*G13,P*[*tubP-GAL80*]*; P*[*TubP-GAL4*]*,P*[*UAS-GFP*]*/+*).

Flip-out clones (Basler and Struhl, 1994) overexpressing Sara (*y*^{1}*w,P*[*hsFLP*]*12/y*^{1}*w,Act>CD2>Gal4; UAS-GFP/+; UAS-HM-Sara/+*) and control clones (*y*^{1}*w,P*[*hsFLP*]*12/y*^{1}*w,Act>CD2>Gal4; UAS-GFP/+; MKRS/+*) were obtained after several crosses. A region of leaky GFP expression was noted in the anterior midgut. Therefore, the analysis of flip-out and also MARCM clones was restricted to the posterior region of the adult midgut.

To induce recombination in both MARCM and flip-out clones, flies were heat-shocked for 20 min at 37°C, on the fifth day following eclosion. Guts were then examined at 10 days post-induction.

Epistasis experiments

Crosses were carried out at permissive temperature (18°C). Control (*w;esg-Gal4,UAS-src-GFP,tubulin-Gal80ts/+*), Sara RNAi (*w;esg-Gal4, UAS-src-GFP,tubulin-Gal80ts/P{GD8765}v19150*), NICD (*w;esg-Gal4, UAS-src-GFP,tubulin-Gal80ts/If; UAS-Notch*^{cdc10}*/+*) and Sara RNAi +NICD (*w;esg-Gal4,UAS-src-GFP,tubulin-Gal80ts/P{GD8765}v19150; UAS-Notch*^{cdc10}*/+*) progeny were grown at 18°C for 4.5 days after hatching and then shifted to restricted temperature (29°C) for 10 days.

Rescue of Sara lethality

Crosses were carried out at 25°C and the total number of flies hatched after 16 days was quantified ($n=420$ flies). Sara lethality was rescued by the expression of Sara-GFP under the control of the ubiquitin promoter. In a genetic cross, we generated siblings corresponding to a Sara loss-of-function mutant genotype, a control heterozygous genotype and a genotype containing rescuing Sara$^+$ transgenes. We obtained only four *Sara* homozygous mutant flies [mutant genotype: *Su(H)GBE-lacZ/+; Df(2R)48,Ubi:Sara-GFP(8.3)/Sara12(1B);MKRS/TM6B*] versus 31 *Sara* heterozygous control flies (control genotype: *Su(H)GBE-lacZ/+; Df(2R)48,Ubi:Sara-GFP(8.3)/CyO,actGFP; MKRS/TM6B*). In the same experiment, 24 'rescue' *Sara* homozygous mutant flies expressing two copies of Ubi:Sara-GFP hatched to adulthood, corresponding to 77% survival [rescue genotype: *Su(H)GBE-lacZ/+; Df(2R) 48,Ubi:Sara-GFP(8.3)/Sara12(1B);MKRS/Ubi:Sara-GFP(15.2)*].

Time-lapse microscopy

Crosses were carried out at 20°C using the temperature-sensitive *esg*^{ts} system. 4.5 days after hatching, progeny were shifted to 29°C for 13 h to suppress the thermosensitive Gal80 inhibitor. Female flies were pinned on a sylgard plate (Sylgard 184 Silicone Elastomer, Dow Corning) and covered with clone 8 medium. Clone 8 medium was generated by supplementing Shield and Sang M3 insect medium (S3652, Sigma) with

Development (2014) 141, 2014-2023 doi:10.1242/dev.104240

2% foetal bovine serum (FBS 10270-098, Invitrogen), 2.5% fly extract and 12.5 units of insulin (I1882, Sigma) per 100 ml. To increase the osmotic pressure of the Clone8 medium to physiological level of 360 mOsm, we added either 0.6 g/l of NaCl (Echalier, 1997) or 0.4 g/l of NaCl and 0.328 g/l $MgCl_2$.

The entire gastrointestinal tract was removed and mounted either on a chamber coverslip containing clone 8 medium and closed by an oxygen-permeable membrane (5794, YSI Incorporated), or on a tissue-culture dish (FD35-100, World Precision Instruments). In this last condition, a clot of fibrin was generated on top of the tissue to maintain it at the bottom of the dish (Loubery and Gonzalez-Gaitan, 2014). The tissue was placed into 20 µl of fibrinogen solution (8 mg/ml, 341573, Calbiochem) and 3 µl of 20 times diluted thrombin protease (27084601, 500 units/ml, GE Healthcare or T9549, 50 units/ml, Sigma) were added carefully before filling the dish with clone 8 medium.

Two-colour movies were generated either with a Zeiss LSM500 microscope using 1 min time and 1 µm step intervals or on a spinning disk microscope using 1 min time and 0.5 µm step intervals. Imaris software was used for image processing.

Infection with *Ecc15* bacteria

Erwinia carotovora carotovora 15 (*Ecc15*) bacteria were grown in 400 ml of LB medium at 29°C overnight. The infection solution was obtained by mixing a volume of concentrated pellet from the overnight culture (optical density OD_{600}=200) with an equal volume of 5% sucrose solution (1:1). For oral infection, 4-day-old flies were starved for 105 min at 29°C in an empty vial before being flipped onto fly medium covered with a filter disk soaked in the infection solution. Flies fed on bacteria for 11 h. Flies were then transferred to fresh vials for 20 min at room temperature before being dissected.

Chloroquine treatment

Flies were grown at room temperature for 13 days. Half of them was then fed on chloroquine solution and the other half ingested a mixture of 10% PBS with 5% sucrose (1:1) for 2 days. The chloroquine solution was obtained by mixing a volume of chloroquine (100 mg/ml, C6628 Sigma in 10% PBS) (Dubois et al., 2001) with 5% sucrose solution (1:1). These solutions (130 µl) were added on a filter disk covering the fly medium and changed every day.

Immunostaining

All the steps were carried out at room temperature. Flies were dissected in clone 8 medium. The dissected gastrointestinal tract was immediately fixed into separate wells of a 24-well tissue culture plate with 4% formaldehyde (F8775, Sigma), in 80 mM Na-Pipes, 5 mM EGTA, 1 mM MgCl2 (PEM) for 10 min and in PEM plus 0.2% Triton X-100 (PEMT) for a further 10 min. Subsequent steps were then carried out in a single well using 0.5 ml of the appropriate solutions unless otherwise specified. Tissues were permeabilized in PEMT for 15 min. They were then washed in PEM plus 50 mM NH_4Cl for 10 min and in PEMT for 10 min. All the next steps were carried out with agitation. Blocking was carried out in 2% normal goat serum (S-1000, Vector Laboratories), 2% BSA in PEMT (0.2 ml) for 1 h. The guts were then incubated with primary antibodies diluted in PEMT plus 2% BSA (0.2 ml) for 2 h. Primary antibodies were removed and samples were rinsed and washed in PEMT for 5×, 10× and 2×15 min, followed by a second blocking. Samples were next incubated with secondary antibodies diluted in a solution of PEMT plus 2% goat serum, 2% BSA (0.2 ml) for 2 h. They were then washed in PEMT for 5×, 10× and 2×15 min, and rinsed in PEM before being mounted in ProLong Gold antifade reagent with DAPI (P36935, Invitrogen).

Antisera

The following primary antibodies were used: mouse monoclonal anti-Delta (1:2000, C594.9B), anti-Prospero (1:100, MR1A), anti-Notch extracellular domain (1:100, C458.2H) and anti-Notch intracellular domain (1:1000, C17.9C6) all from Developmental 8 Studies Hybridoma Bank; rabbit polyclonal anti-phospho-Histone H3 (PH3) (1:500, H9161, Sigma); rabbit polyclonal anti-β-Galactosidase (pre-absorbed against *Drosophila* embryos and used at 1:500, 55976, Cappel); and rat polyclonal anti-GFP (1A5, 1:500, sc-101536), rabbit polyclonal anti-armadillo (Arm) (d-300, 1:100, sc-28653) and goat polyclonal anti-dsRed (L-18, 1:100, sc-33353) all from Santa Cruz.

Anti-β-tubulin antibody was obtained by purifying E7 monoclonal antibody from hybridoma supernatant on a protein G column. Purified antibody was then covalently coupled with Alexa 488 (Molecular Probes) by NHS chemistry followed by free dye removal using gel filtration on a G-25 column in PBS. Degree of labelling was measured at 0.8 (E. Derivery, University of Geneva, Geneva, Switzerland).

Secondary antibodies were used at 1:500 and were either goat or donkey IgG (anti-mouse, anti-rabbit, anti-rat and anti-goat) conjugated to either Alexa 488, Alexa 546, Alexa Cy5 or Alexa 647 (Molecular Probes). DNA was labelled with DAPI contained in ProLong Gold antifade reagent (P36935, Invitrogen).

Quantification

Quantification of Sara endosome quantity in dividing ISCs at prophase was carried out using ImageJ software. Three-dimensional confocal stacks were first processed using a wavelet 'a trous' filter in order to enhance the detection of small and dim vesicles ('ImproveKymo' ImageJ plug-in, developed by F. Cordelières, Institut Curie, Orsay, France). Three-dimensional segmentation was then performed using the '3D object counter' ImageJ plug-in (Bolte and Cordelieres, 2006), keeping the intensity threshold constant for all the cells. The results are expressed as the mean of detected objects per dividing cell, corresponding to the number of Sara endosomes. The same software has been used to measure the volumetric ratio of Sara endosomes in the EB compared with the total endosomal volume.

Quantification of Sara endosome enrichment in each daughter cell was carried out using the ImageJ software. In image stacks of dividing ISCs at early cytokinesis, the threshold was adjusted not to take into account the cytoplasmic signal background and to still detect the smallest endosomal structures. For each stack, areas were delimited in which all endosomes of one future daughter cell were present. The sum of pixel intensities in drawn areas was then measured. The ratio of endosomes between the two future daughter cells was obtained by dividing the quantity of Sara endosomes contained in the daughter cell receiving the biggest amount by the quantity found in its sibling. Moreover, the percentage of Sara endosome enrichment in one particular daughter cell was calculated by dividing the raw integrated density in this cell by the total raw integrated density for the two daughters.

The colocalization between Sara endosomes and Delta/Notch positive endocytic vesicles was measured by particle image cross-correlation spectroscopy (PICCS), as previously described (Semrau et al., 2011). The pixel size in each confocal section was equal to 0.06 µm. The background was removed by applying a low-pass filter and subtracting it from the original image with a cut-off of one pixel. Endosomes were detected using an adaptive threshold as previously described (Keller et al., 2008).

Calculation of the ISC cell cycle length

The total number of ISCs and dividing stem cells per clone has been determined by Delta and PH3 immunostaining, respectively. The ratio of PH3-positive cells versus the total number of Delta-positive cells in clones corresponds to the mitotic index. As ISCs do not divide in synchrony, the probability of finding a cell in mitosis is equal to the duration of mitosis divided by the duration of the cell cycle length. As the duration of mitosis is robustly constant (around 2 h), we can use the mitotic index as a proxy to calculate the cell cycle length (2 h multiplied by the inverse of the mitotic index). The mitotic index in control clones (*mi*=3.4%) is sevenfold higher than in Sara mutant clones (*mi*=0.5%).

Statistical analysis

Sigmastat software was used to test the normality and the equal variance for pooled data, as well as to run statistical tests. All results are presented as mean±s.e.m. Statistical tests used in each experiment are specified in the legend of the figure.

Acknowledgements
We thank N. Buchon, S. Loubéry, L. Holtzer, M. Derivery, D. Osman, C. Seum and the bioimaging platform for reagents and technical help. We are grateful to A. Martinez-Arias, J. de Navascués and B. Lemaitre for critical reading of the manuscript and helpful discussions.

Competing interests
The authors declare no competing financial interests.

Author contributions
C.M performed the experiments; C.M and M.G.-G. wrote the manuscript.

Funding
This work was supported by the Departement d'Instruction Publique of the Canton of Geneva, the Swiss National Science Foundation, the European Research Council Grant (Sara), the Polish–Swiss research programme, the systemsX grant EpiphysX and the National Center of Competence in Research Chemical Biology programmes. Deposited in PMC for immediate release.

Supplementary material
Supplementary material available online at
http://dev.biologists.org/lookup/suppl/doi:10.1242/dev.104240/-/DC1

References

Atwood, S. X. and Prehoda, K. E. (2009). aPKC phosphorylates Miranda to polarize fate determinants during neuroblast asymmetric cell division. *Curr. Biol.* **19**, 723-729.
Bardin, A. J., Perdigoto, C. N., Southall, T. D., Brand, A. H. and Schweisguth, F. (2010). Transcriptional control of stem cell maintenance in the Drosophila intestine. *Development* **137**, 705-714.
Basler, K. and Struhl, G. (1994). Compartment boundaries and the control of Drosopfiffa limb pattern by hedgehog protein. *Nature* **368**, 208-214.
Bennett, D. and Alphey, L. (2002). PP1 binds Sara and negatively regulates Dpp signaling in Drosophila melanogaster. *Nat. Genet.* **31**, 419-423.
Bokel, C., Schwabedissen, A., Entchev, E., Renaud, O. and Gonzalez-Gaitan, M. (2006). Sara endosomes and the maintenance of Dpp signaling levels across mitosis. *Science* **314**, 1135-1139.
Bolte, S. and Cordelieres, F. P. (2006). A guided tour into subcellular colocalization analysis in light microscopy. *J. Microsc.* **224**, 213-232.
Brennan, K., Tateson, R., Lieber, T., Couso, J. P., Zecchini, V. and Arias, A. M. (1999). The abruptex mutations of notch disrupt the establishment of proneural clusters in Drosophila. *Dev. Biol.* **216**, 230-242.
Buchon, N., Broderick, N. A., Chakrabarti, S. and Lemaitre, B. (2009). Invasive and indigenous microbiota impact intestinal stem cell activity through multiple pathways in Drosophila. *Genes Dev.* **23**, 2333-2344.
Coumailleau, F., Fürthauer, M., Knoblich, J. A. and González-Gaitán, M. (2009). Directional Delta and Notch trafficking in Sara endosomes during asymmetric cell division. *Nature* **458**, 1051-1055.
de Navascués, J., Perdigoto, C. N., Bian, Y., Schneider, M. H., Bardin, A. J., Martínez-Arias, A. and Simons, B. D. (2012). Drosophila midgut homeostasis involves neutral competition between symmetrically dividing intestinal stem cells. *EMBO J.* **31**, 2473-2485.
Dubois, L., Lecourtois, M., Alexandre, C., Hirst, E. and Vincent, J.-P. (2001). Regulated endocytic routing modulates wingless signaling in Drosophila embryos. *Cell* **105**, 613-624.
Echalier, G. (1997). *Drosophila Cells in Culture*. London, UK: Academic Press.
Furriols, M. and Bray, S. (2001). A model Notch response element detects Suppressor of Hairless-dependent molecular switch. *Curr. Biol.* **11**, 60-64.
Fürthauer, M. and González-Gaitán, M. (2009a). Endocytosis, asymmetric cell division, stem cells and cancer: unus pro omnibus, omnes pro uno. *Mol. Oncol.* **3**, 339-353.
Fürthauer, M. and González-Gaitán, M. (2009b). Endocytic regulation of notch signalling during development. *Traffic* **10**, 792-802.
Goulas, S., Conder, R. and Knoblich, J. A. (2012). The Par complex and integrins direct asymmetric cell division in adult intestinal stem cells. *Cell Stem Cell* **11**, 529-540.
Guo, Z., Driver, I. and Ohlstein, B. (2013). Injury-induced BMP signaling negatively regulates Drosophila midgut homeostasis. *J. Cell Biol.* **201**, 945-961.
Hsu, Y.-C. and Fuchs, E. (2012). A family business: stem cell progeny join the niche to regulate homeostasis. *Nat. Rev. Mol. Cell Biol.* **13**, 103-114.
Itoh, F., Divecha, N., Brocks, L., Oomen, L., Janssen, H., Calafat, J., Itoh, S. and ten Dijke, P. (2002). The FYVE domain in Smad anchor for receptor activation (SARA) is sufficient for localization of SARA in early endosomes and regulates TGF-beta/Smad signalling. *Genes Cells* **7**, 321-331.
Johnson, K. G., Ghose, A., Epstein, E., Lincecum, J., O'Connor, M. B. and Van Vactor, D. (2004). Axonal heparan sulfate proteoglycans regulate the distribution and efficiency of the repellent slit during midline axon guidance. *Curr. Biol.* **14**, 499-504.
Kawaguchi, D., Furutachi, S., Kawai, H., Hozumi, K. and Gotoh, Y. (2013). Dll1 maintains quiescence of adult neural stem cells and segregates asymmetrically during mitosis. *Nat. Commun.* **4**, 1880.
Keller, P. J., Schmidt, A. D., Wittbrodt, J. and Stelzer, E. H. K. (2008). Reconstruction of zebrafish early embryonic development by scanned light sheet microscopy. *Science* **322**, 1065-1069.
Lee, T. and Luo, L. (1999). Mosaic analysis with a repressible cell marker for studies of gene function in neuronal morphogenesis. *Neuron* **22**, 451-461.
Lee, C.-Y., Robinson, K. J. and Doe, C. Q. (2006). Lgl, Pins and aPKC regulate neuroblast self-renewal versus differentiation. *Nature* **439**, 594-598.
Loubéry, S. and González-Gaitán, M. (2014). Monitoring notch/delta endosomal trafficking and signaling in Drosophila. *Methods Enzymol.* **534**, 301-321.
Lu, B., Rothenberg, M., Jan, L. Y. and Jan, Y. N. (1998). Partner of Numb colocalizes with Numb during mitosis and directs Numb asymmetric localization in Drosophila neural and muscle progenitors. *Cell* **95**, 225-235.
Mayer, B., Emery, G., Berdnik, D., Wirtz-Peitz, F. and Knoblich, J. A. (2005). Quantitative analysis of protein dynamics during asymmetric cell division. *Curr. Biol.* **15**, 1847-1854.
Micchelli, C. A. and Perrimon, N. (2006). Evidence that stem cells reside in the adult Drosophila midgut epithelium. *Nature* **439**, 475-479.
Morrison, S. J. and Spradling, A. C. (2008). Stem cells and niches: mechanisms that promote stem cell maintenance throughout life. *Cell* **132**, 598-611.
O'Brien, L. E., Soliman, S. S., Li, X. and Bilder, D. (2011). Altered modes of stem cell division drive adaptive intestinal growth. *Cell* **147**, 603-614.
Ohlstein, B. and Spradling, A. (2006). The adult Drosophila posterior midgut is maintained by pluripotent stem cells. *Nature* **439**, 470-474.
Ohlstein, B. and Spradling, A. (2007). Multipotent Drosophila intestinal stem cells specify daughter cell fates by differential notch signaling. *Science* **315**, 988-992.
Perdigoto, C. N. L. R., Gervais, L., Overstreet, E., Fischer, J., Guichet, A. and Schweisguth, F. (2008). Overexpression of partner of numb induces asymmetric distribution of the PI4P 5-Kinase Skittles in mitotic sensory organ precursor cells in Drosophila. *PloS ONE* **3**, e3072.
Perdigoto, C. N., Schweisguth, F. and Bardin, A. J. (2011). Distinct levels of Notch activity for commitment and terminal differentiation of stem cells in the adult fly intestine. *Development* **138**, 4585-4595.
Roegiers, F., Younger-Shepherd, S., Jan, L. Y. and Jan, Y. N. (2001). Bazooka is required for localization of determinants and controlling proliferation in the sensory organ precursor cell lineage in Drosophila. *Proc. Natl. Acad. Sci. U.S.A.* **98**, 14469-14474.
Semrau, S., Holtzer, L., González-Gaitán, M. and Schmidt, T. (2011). Quantification of biological interactions with particle image cross-correlation spectroscopy (PICCS). *Biophys. J.* **100**, 1810-1818.
Snippert, H. J., van der Flier, L. G., Sato, T., van Es, J. H., van den Born, M., Kroon-Veenboer, C., Barker, N., Klein, A. M., van Rheenen, J., Simons, B. D. et al. (2010). Intestinal crypt homeostasis results from neutral competition between symmetrically dividing Lgr5 stem cells. *Cell* **143**, 134-144.
Spana, E. P. and Doe, C. Q. (1996). Numb antagonizes Notch signaling to specify sibling neuron cell fates. *Neuron* **17**, 21-26.
Stenmark, H. and Aasland, R. (1999). FYVE-finger proteins–effectors of an inositol lipid. *J. Cell Sci.* **112**, 4175-4183.
Takashima, S., Adams, K. L., Ortiz, P. A., Ying, C. T., Moridzadeh, R., Younossi-Hartenstein, A. and Hartenstein, V. (2011). Development of the Drosophila entero-endocrine lineage and its specification by the Notch signaling pathway. *Dev. Biol.* **353**, 161-172.
Tsukazaki, T., Chiang, T. A., Davison, A. F., Attisano, L. and Wrana, J. L. (1998). SARA, a FYVE domain protein that recruits Smad2 to the TGFbeta receptor. *Cell* **95**, 779-791.
Wang, H., Ouyang, Y., Somers, W. G., Chia, W. and Lu, B. (2007). Polo inhibits progenitor self-renewal and regulates Numb asymmetry by phosphorylating Pon. *Nature* **449**, 96-100.
Wirtz-Peitz, F., Nishimura, T. and Knoblich, J. A. (2008). Linking cell cycle to asymmetric division: Aurora-A phosphorylates the Par complex to regulate Numb localization. *Cell* **135**, 161-173.